Nitric Oxide 93 (2019) 78–89

Contents lists available at ScienceDirect

Nitric Oxide

journal homepage: www.elsevier.com/locate/yniox

Nitric oxide stimulates a PKC-Src-Akt signaling axis which increases human immunodeficiency virus type 1 replication in human T lymphocytes

Marli F. Curcio[a,*], Wagner L. Batista[b,c], Eloísa D. Castro[d], Scheilla T. Strumillo[d], Fernando T. Ogata[e], Wagner Alkmim[b], Milena K.C. Brunialti[a], Reinaldo Salomão[a], Gilberto Turcato[a], Ricardo S. Diaz[a], Hugo P. Monteiro[d], Luiz Mário R. Janini[a,b]

[a] Department of Medicine/Infectious Diseases, Universidade Federal de São Paulo, São Paulo, Brazil
[b] Department of Microbiology, Immunology and Parasitology, Universidade Federal de São Paulo, São Paulo, Brazil
[c] Department of Pharmaceutical Sciences, Universidade Federal de São Paulo, Diadema, Brazil
[d] Department of Biochemistry/Molecular Biology, CTCMol, Universidade Federal de São Paulo, Brazil
[e] Structural and Functional Ecology of Ecosystems, Universidade Paulista, Sorocaba, Brazil

ARTICLE INFO

Keywords:
Oxidative stress
Cellular redox status
Nitric oxide
Src kinase
HIV
Viral load

ABSTRACT

Human immunodeficiency virus (HIV) infections are typically accompanied by high levels of secreted inflammatory cytokines and generation of high levels of reactive oxygen species (ROS). To elucidate how HIV-1 alters the cellular redox environment during viral replication, we used human HIV-1 infected $CD4^+$T lymphocytes and uninfected cells as controls. ROS and nitric oxide (NO) generation, antioxidant enzyme activity, protein phosphorylation, and viral and proviral loads were measured at different times (2–36 h post-infection) in the presence and absence of the NO donor S-nitroso-N-acetylpenicillamine (SNAP). HIV-1 infection increased ROS generation and decreased intracellular NO content. Upon infection, we observed increases in copper/zinc superoxide dismutase (SOD1) and glutathione peroxidase (GPx) activities, and a marked decrease in glutathione (GSH) concentration. Exposure of HIV-1 infected $CD4^+$T lymphocytes to SNAP resulted in an increasingly oxidizing intracellular environment, associated with tyrosine nitration and SOD1 inhibition. In addition, SNAP treatment promoted phosphorylation and activation of the host's signaling proteins, PKC, Src kinase and Akt. Inhibition of PKC leads to inhibition of Src kinase strongly suggesting that PKC is the upstream element in this signaling cascade. Changes in the intracellular redox environment after SNAP treatment had an effect on HIV-1 replication as reflected by increases in proviral and viral loads. In the absence or presence of SNAP, we observed a decrease in viral load in infected $CD4^+$T lymphocytes pre-incubated with the PKC inhibitor GF109203X. In conclusion, oxidative/nitrosative stress conditions derived from exposure of HIV-1-infected $CD4^+$T lymphocytes to an exogenous NO source trigger a signaling cascade involving PKC, Src kinase and Akt. Activation of this signaling cascade appears to be critical to the establishment of HIV-1 infection.

1. Introduction

Human immunodeficiency virus (HIV) infections are typically accompanied by chronic microinflammation and T-cell activation with high levels of inflammatory cytokine secretion, and high levels of intracellular generation of ROS [1,2]. The underlying persistent oxidative stress yields an imbalance of intracellular antioxidant defenses. Decreased glutathione (GSH) and thioredoxin (Trx) levels have been consistently reported during HIV-1 infection [3–7]. Thus, the use of antioxidants to reduce ROS levels in HIV-infected patients has been extensively examined [8–11].

The imbalance between ROS production and elimination during HIV-1 infection is well established [12,13]. Several groups have demonstrated these events either by measuring H_2O_2 production and viral load, or by comparing the regulation of transcription factors (e.g., NF-κB) during the interplay between ROS production and HIV-1 replication [14,15]. These results suggest that distinct pathways regulate ROS turnover with a direct impact on HIV-1 replication [12,16,17]. In addition, the signaling free radical nitric oxide (NO) also plays an important, albeit dual role in HIV-1 infection. NO may be beneficial to the

* Corresponding author. Department of Medicine/Infectious Diseases Universidade Federal de São Paulo, Rua Pedro de Toledo, 781, Zip code: 04039-032, São Paulo, Brazil.
E-mail address: curcio@unifesp.br (M.F. Curcio).

https://doi.org/10.1016/j.niox.2019.09.004
Received 7 September 2018; Received in revised form 12 August 2019; Accepted 16 September 2019
Available online 17 September 2019
1089-8603/

host through inhibition of viral enzymes or damaging through activation of cellular signaling proteins that will support viral replication [18–21].

The pathogenic effects of NO-mediated events depend upon the formation of secondary intermediates, such as peroxynitrite anion ($ONOO^-$) and nitrogen dioxide (NO_2), which are more reactive than NO itself [22–24]. The interplay between ROS and NO is involved in normal and pathological conditions primarily through nitration of tyrosine residues on target proteins [18].

A recent study analyzed human brains from individuals who had HIV infection without encephalitis and with encephalitis, and compared both groups to brains of healthy individuals. Nitrated proteins were predominantly found in HIV-infected individuals with encephalitis [25].

Cairoli and co-workers [26] showed that in peripheral blood mononuclear cells (PBMCs) from HIV-infected patients there is a significant decrease in NO production and inducible nitric oxide synthase (iNOS) mRNA expression. A decrease in NO levels during infection may favor disease progression, possibly due to the loss of antiviral and anti-apoptotic activities [26].

The cellular redox state in lymphocytes may be modulated by endogenous generation of ROS and NO. These reactive species can interfere with the biochemical parameters of cell activation [27,28]. Furthermore, exogenously supplied oxidants, such as haemin and the NO donors sodium nitroprusside (SNP) and SNAP, stimulate tyrosine phosphorylation and regulate signaling pathways in fibroblasts, endothelial cells and lymphocytes [29–31]. However, the redox regulation of signaling pathways triggered by HIV infection is poorly understood.

In the present study, we analyzed ROS/NO production and antioxidant cellular defenses in response to HIV-1 infection in $CD4^+$T lymphocytes obtained from healthy individuals, in the presence and absence of SNAP. Infected cells showed lower NO production and higher ROS and antioxidant enzyme levels compared to uninfected cells. Analysis of the redox pair GSH/GSSG (reduced glutathione/glutathione disulfide) suggested the presence of an oxidizing intracellular redox environment in infected cells that was probably a consequence of viral infection. Exposure of infected cells to SNAP resulted in inhibition of ROS production and SOD1 activity. ROS production and SOD1 activity were higher in infected cells without SNAP treatment. Furthermore, HIV-1 infection of $CD4^+$T lymphocytes resulted in changes in the phosphorylation levels of PKC, Src kinase and Akt. Exposure of HIV-1-infected $CD4^+$T lymphocytes to SNAP stimulated the PKC, Src kinase and Akt signaling axis with major consequences for viral load and viral integration.

2. Materials and methods

2.1. Materials

The chemical reagents, 5,5′-dithiobis-2-nitrobenzoic acid (DTNB), reduced form of glutathione (GSH), disulfide form of glutathione (GSSG), glutathione reductase (GR), NADPH, sulfosalicylic acid, triethanolamine and 2-vinylpyridine, were obtained from Sigma Aldrich (St. Louis, MO, USA). GF109203X was obtained from Tocris Bioscience (Bristol, United Kingdom) and kindly supplied by Dr. Edgar Paredes Gamero, 2-(4-carboxyphenyl)-4,4,5,5-tetramethylimidazoline-1-oxyl-3-oxide (cPTIO) was obtained from Cayman Chemicals (Ann Arbor, Michigan, USA). The antibodies against phospho-Src Tyr^{416}, SOD1, phospho-PKC (pan Thr^{514}), Akt and phospho-Akt Ser^{473} were obtained from Cell Signaling Technologies (Beverly, MA, USA). The antibodies against Src kinase and PKC were obtained from Merck-Millipore (Lake Placid, NY, USA). Mouse monoclonal and rabbit polyclonal secondary antibodies conjugated with HRP were purchased from GE Healthcare (GE Healthcare, UK). The Super Signal substrate used to develop the Western blots was obtained from Pierce (Rockford, IL, USA). S-Nitroso-N-acetylpenicillamine (SNAP), dichloro-dihydrofluorescein diacetate (DCFH-DA) and 4-amino-5-methylamino-2,7′-difluorescein diacetate (DAF-2DA) were obtained from Calbiochem (San Diego, CA, USA).

2.2. Cell cultures

This study was performed according to the protocol of the UNIFESP Ethics Committee - 0599/10. Whole blood of healthy donors was provided by the Charitable Association of Blood Collection - COLSAN, São Paulo, Brazil. Peripheral blood mononuclear cells (PBMCs) were separated from whole blood according to the standard separation protocol using Ficoll-Paque Plus (GE, Marborough, MA, USA). PBMCs were maintained in RPMI 1640 medium supplemented with 1% penicillin/streptomycin and 10% fetal bovine serum (FBS) in a 5% CO_2 incubator at 37 °C. At 48 h prior to infection, PBMCs were stimulated with 0.03 μg/mL of phytohemagglutinin. $CD4^+$T lymphocytes were isolated from phytohemagglutinin-stimulated PBMCs (EasySep Human $CD4^+$ Positive Selection; Stem Cell, Vancouver, BC, Canada) and 10 IU/mL of interleukin-2 (Hoffmann-La Roche AG, Basel, Switzerland) was added to the cell suspension prior to experimental infection. HeLa cells were maintained in MEM supplemented with 1% penicillin/streptomycin and 10% FBS in a 5% CO_2 incubator at 37 °C.

2.3. Cell viability assay

One hundred thousand $CD4^+$T lymphocytes per well were seeded in a 12-well culture plate and incubated with SNAP at increasing concentrations: 0.1, 0.15, 0.2 and 0.25 mM. SNAP was added to cell cultures every 10 h over a period of 36 h at 37 °C. Cell viability was evaluated by trypan blue staining. Experiments were performed in triplicate.

2.4. Estimation of intracellular generation of NO and nitrosated species (NOx)

Relative fluorescence intensities that reflect the intracellular generation of NO and nitrosated species [32] are plotted against the two concentrations of SNAP (0.1 or 0.2 mM) in the presence or absence of 30 μM cPTIO using ten thousand $CD4^+$T lymphocytes/well seeded in a 96-well cultureincubated with 5 μM DAF-2 DA. Excitation wavelength was set at 485 nm, and emission wavelength was set at 515 nm. Fluorescence intensities were normalized based on the number of cells per sample. Unlabeled samples were used as blanks. Experiments were performed five times.

2.5. Measurements of intracellular ROS production

HIV-1-induced ROS production in cells was analyzed by flow cytometry using the Guava cytometer (Merck-Millipore, Lake Placid, NY, USA). At each experimental time point, 10 μM DCFH-DA was added directly to the medium and cells were incubated at 37 °C for 30 min. Following incubation and washing, the intracellular fluorescence of DCFH was analyzed by flow cytometry. The data were analyzed using the InCyte software (version 8/8HT).

2.6. Quantitative determination of GSH and GSSG

$CD4^+$T lymphocytes were lysed in lysis buffer A. After lysis, the cells were centrifuged at 12,000 × *g* for 10 min at 4 °C. The supernatant was immediately transferred to 1.5 mL tubes and stored at −80 °C. GSH and GSSG concentrations were determined essentially as described by Rahman [33]. After obtaining the GSH and GSSG concentrations, the values were used as reference values for the cellular redox environment.

2.7. Glutathione peroxidase (GPx) activity assay

A total of 20 μg of protein obtained from cell lysates was used to determine GPx activity. Total GPx activity was determined using tert-butyl hydroperoxide (1.2 mM) as the substrate. Absorbance at 340 nm was monitored for 5 min in 100 mM phosphate buffer (pH 7.0) and 1 mM EDTA at 37 °C. One unit of activity is defined as the amount of protein capable of oxidizing 1 mM NADPH per minute and is expressed as U/mg of protein [34].

2.8. Glutathione reductase (GR) activity assay

A total 50 μL cell lysate sample was used to determine GR activity as previously described [35]. Total activity was determined using a 1 mL mixture containing 1.0 mM GSSG, 0.1 mM NADPH, 0.5 mM EDTA, 0.10 mM sodium phosphate buffer (pH 7.6) and 250 U/mL of the GR sample to obtain a change in absorbance of 0.05–0.3/min. The oxidation of 1 μmol of NADPH/min under these conditions was used as the unit of GR activity. Specific activity is expressed as units per mg of protein.

2.9. SOD1 activity assay

The complete reaction solution (250 μL) consisted of 50 mM phosphate buffer (pH 7.4) containing 0.1 mM EDTA, 62 μM nitroblue tetrazolium (NBT), 98 μM NADH and 3.3 μM phenazine methosulfate. For the assay, a 25 μL test sample was pipetted into a microtiter well containing 200 μL of freshly prepared buffer. Absorbance was measured at 560 nm for 3 min in 30s steps to create an index of NBT reduction using a SpectraMax 250 microplate reader (Molecular Devices, Sunnyvale, CA, USA) in the kinetic mode with the “automix” function activated. Alternatively, measurements of absorbance at 560 nm were obtained after 5 min of incubation. SOD1 activity from cell lysates was expressed in units of SOD/mg, where 1 unit is the amount of SOD required to give 50% maximum inhibition of the initial rate of NBT reduction [36].

2.10. Virus stock preparation and cellular infection

To produce virus particles, HeLa cells were transfected with the infectious molecular clone pNL4-3 (AIDS Reagent Program, NIH, USA, cat. number 114) using the Effectene Reagent (QIAGEN, Germany) according to the manufacturer's protocol. After 72 h of transfection, supernatants containing the virus were harvested by centrifugation during 5 min at 2,000 × *g*, filtered through a 0.45 μm pore-sized filter (Sartorius, Goettingen, Germany), aliquoted and frozen at −80 °C. RNA viral loads were quantified by real-time PCR (Abbot M2000 Real-Time System, IL, USA) according to the manufacturer's instructions. A multiplicity of infection (MOI) of 0.1 was used for infection of isolated $CD4^+$T lymphocytes. *In vitro* infection was performed according to Mohammadi et al. [37]. Briefly, cells were incubated for 72 h, and harvested at the time points of 2, 12, 24, 36 and 72 h (post infection). Cell culture supernatants were collected at the same time points. The time points correspond to different viral infection stages. After attachment of the virus to the plasma membrane of $CD4^+$T lymphocytes, redox alterations were evaluated at three different viral infection stages: (1) At 2 h in the cytoplasm, corresponding to an early stage; (2) At 12 h in the nucleus, corresponding to a middle stage; (3) At 24 and 36 h in the cytoplasm, corresponding to late stages. At 36 h viral proteins are translated and particles are assembled and start to bud from the cells (Fig. 1A). The experiments were performed in triplicate.

2.11. Total viral DNA quantification

For DNA quantification, infected $CD4^+$T lymphocytes were collected during the three stages described above and DNA was extracted using the DNA Blood Mini Kit (QIAGEN, Germany) according to the manufacturer's protocol. Extracted DNA was used as the template for qPCR following the TaqMan method to generate a 203 bp amplicon from the HIV-1 integrase gene (nucleotides 4309–4511 according to the viral isolate HXB2). The reaction had a final volume of 50 μL and consisted of 1x GoldStar PCR Buffer (Promega, WI, USA), 3.5 mM $MgCl_2$, 0.4 mM dNTPs, 400 nM of each primer (Int-F (5′ ACC TGC CTG TAG CAC CAA A 3′) and Int-R (5′ CTG CCC TGT TTC TGG TGC AAT AAC 3′)), 200 nM of the HIV-1 integrase probe (5′ FAM-TGG TTC TAG CAG ATG CCA GTG TAG GA-TAMRA 3′), 0.5 U/μL of Platinum® Taq DNA Polymerase (Invitrogen, USA) and 5 μL of DNA. Amplification was performed using the iCycler PCR System 7700 (Bio-Rad, CA, USA) under the following conditions: initial denaturation at 94 °C for 5 min, followed by 45 amplification cycles with denaturation at 94 °C for 20 s and annealing and extension at 60 °C for 1 min. The human serum albumin gene was used as the endogenous control to quantify the total cell number in each sample. The primers used for albumin were Alb-F (5′ GCT GTC ATC TGT TCT GGG CTG T 3′) and Alb-R (5′ CTC AAA ATG GCT GCT GGT GGA T 3′) and the probe was HEX-Alb (5′ HEX-CCT GTC CCC ACA ATG CAA ATC TCT CC 3′BHQ_2/-3 ′) [38].

2.12. Viral load quantification

HIV-1 viral load was quantified by Abbott Real-Time HIV-1 RT-PCR with the automated 2000 System (IL, USA). Viral RNA was quantified within the dynamic range for detection between 1×10^7 to 4×10^8 RNA copies/mL.

2.13. Immunoblotting

$CD4^+$T lymphocytes were lysed in lysis buffer A (20 mM HEPES (pH 7.5), 150 mM NaCl, 10% glycerol, 1% Triton X-100, 1.5 mM $MgCl_2$, 1 mM EGTA, 1 μg/mL of aprotinin, 1 μg/mL of leupeptin, 1 mM PMSF and phosphatase inhibitors, 2 mM sodium orthovanadate, 50 mM NaF and 10 mM sodium pyrophosphate). Total cell lysates (100 μg of protein/lane) were resolved in 10% sodium dodecyl sulfate (SDS) polyacrylamide gels. Gels were blotted onto nitrocellulose membranes and probed with monoclonal or polyclonal antibodies against the proteins SOD1, Src kinase, Src phospho-Tyr^{416}, PKC, PKC phospho-(pan) gamma Thr^{514}, Akt and Akt phospho-Ser^{473}. After incubation with the appropriate horseradish peroxidase (HRP)-conjugated secondary antibodies, blots were developed using the Super Signal system and digitally registered on LAS-4000 (Fujifilm, Tokyo, Japan).

2.14. Immunoprecipitation

For the immunoprecipitation analysis, the lysates were incubated at 4 °C with the anti-nitro-Tyr antibody overnight on a rotator. Then, 50 μL of protein G agarose beads were added and incubated at 4 °C for 2 h on a rotator. The beads were centrifuged at 10,000 × *g* for 3 min at 4 °C. The supernatant was discarded and beads were washed 3 times in PBS, resuspended in 2x gel loading buffer, and boiled for 5 min prior to separation using SDS–polyacrylamide gel electrophoresis. The separated proteins were transferred onto nitrocellulose membranes, and immunoblotting was performed using anti-SOD as the primary antibody. After incubation with the appropriate HRP-conjugated secondary antibody, blots were developed using the Super Signal system (Thermo-Pierce, Rockford, IL, USA) and digitally registered on LAS-4000 (Fujifilm, Tokyo, Japan).

2.15. Statistical analysis

Statistical analysis was performed using GraphPad Prism version 7.0 (GraphPad Software, San Diego, CA, USA). The differences between the infected and non-infected groups with or without SNAP treatment were examined by Student's t-test. One sample *t*-test and two-way ANOVA were performed and followed by Sidak's multiple comparisons test.

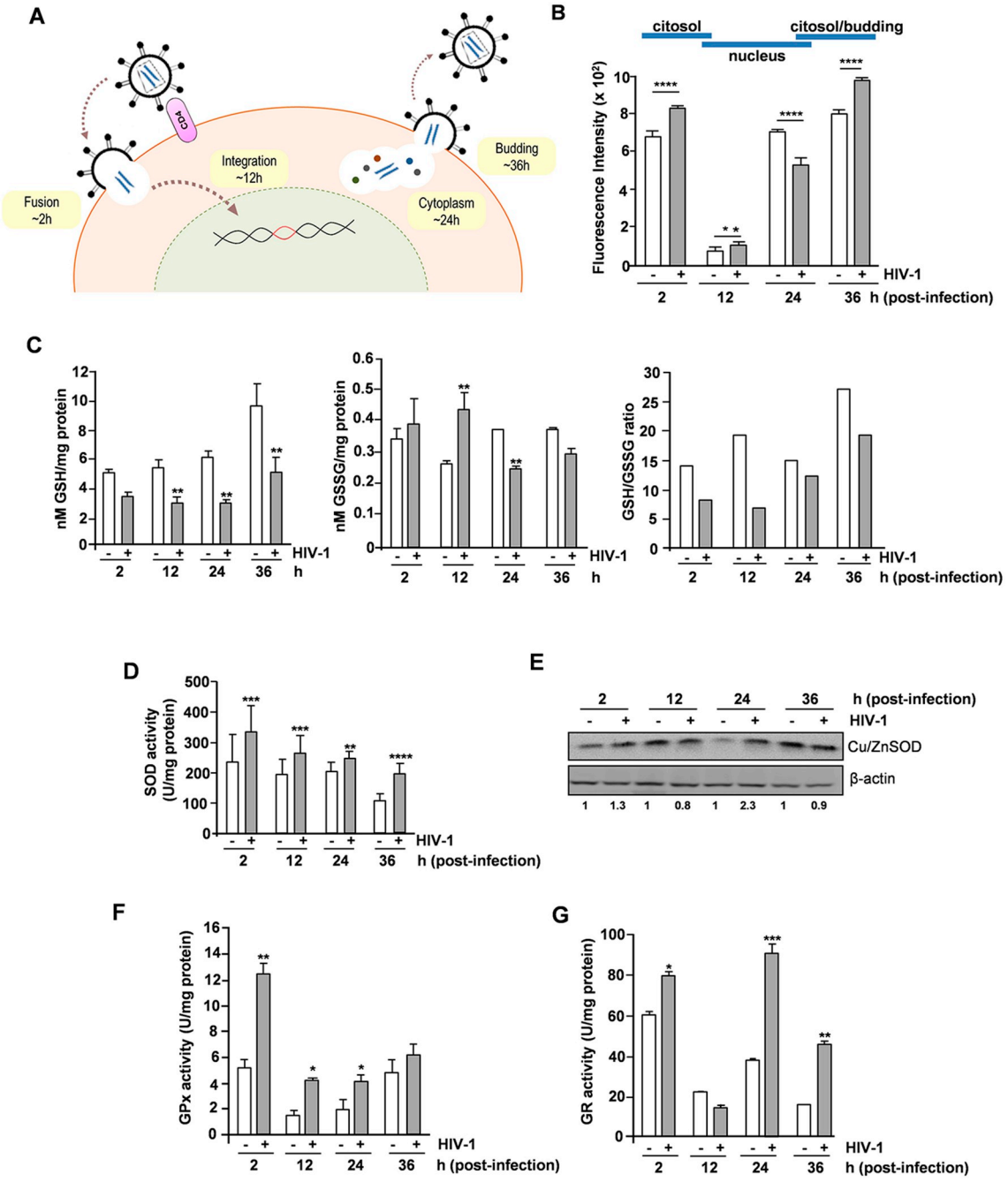

Fig. 1. The impact of HIV-1 infection in the cellular redox environment in CD4$^+$ T lymphocytes. (A) HIV replication cycle. After virus attachment to the cell membrane, redox alterations were evaluated at three different stages: (1) at 2 h in the cytoplasm, corresponding to the early stage of the replication cycle; (2) at 12 h in the nucleus, corresponding to viral integration and synthesis of viral mRNAs; (3) at 24 and 36 h in the cytoplasm, corresponding to late stages. At 36 h, viral proteins are being translated and particles are assembled and start to bud from the cells (figure adapted from Mohammadi et al., 2013). (**B**) Cells were seeded into twenty-four-well plates and infected with HIV-1. ROS production was analyzed at different time points post-infection. This analysis was performed by incubating the cells with DCFH-DA for 30 min prior to measuring intracellular ROS production by infected and non-infected CD4$^+$ T lymphocytes on a flow cytometer. (**C**) Quantification of GSH (left), GSSG (middle) and the GSH/GSSG ratio (right panel in infected and non-infected CD4$^+$ T lymphocytes. The GSH/GSSG ratios (right panel) are the GSH levels divided by the GSSG levels. (**D**) A Cu/ZnSOD enzymatic activity assay was performed at different time points after HIV-1 infection of CD4$^+$ T lymphocytes. Sidak's multiple comparisons test was used for statistical comparisons, and the observed differences were statistically significant. Error bars represent three independent experiments and are represented by the mean ± SD (**$p < 0.01$ and ***$p < 0.001$). (**E**) Representative Western blot showing Cu/ZnSOD expression, performed in infected and non-infected CD4$^+$ T lymphocytes. The values below the images correspond to the relative measurement obtained. The enzymatic activity assay was performed at different time points after HIV-1 infection of CD4$^+$ T lymphocytes. The Western blot is representative for three independent experiments. GPx (**F**) or GR (**G**) enzymatic activity was assessed in infected and non-infected CD4$^+$ T cells. All of the data shown in this figure were analyzed using Sidak's multiple comparisons test. Error bars correspond to the standard deviations (SD) of the measurements made in triplicate (*$p < 0.05$, **$p < 0.01$, ***$p < 0.001$ and ****$p < 0.0001$).

Graphs were represented by the mean ± standard deviation (SD). Differences were considered significant at $p < 0.05$ and represented by * $p < 0.05$, ** $p < 0.01$, *** $p < 0.001$ and **** $p < 0.0001$.

3. Results

3.1. HIV-1 infection affects the intracellular levels of ROS and modulates the host's antioxidant defenses

$CD4^+$T lymphocytes are the main target cells from the beginning of HIV-1 infection up to full development of Acquired Immunodeficiency Syndrome (AIDS). Elevated ROS levels have been associated early on with the progression of HIV-1 infection [39]. We examined whether HIV-1 infection modulates ROS generation in freshly isolated human $CD4^+$T lymphocytes. Our results show that ROS production was significantly increased at 2 and 36 h ($p < 0.0001$) but decreased at 24 h ($p < 0.0001$), post-infection (Fig. 1B).

HIV-1 infection modulates the intracellular antioxidant systems of the host. Changes in intracellular GSH levels and in activities of the antioxidant enzymes SOD1, (GPx) and glutathione reductase (GR) have been previously reported [40–43].

HIV-1-infected patients exhibit GSH depletion as an important marker of disease progression [44]. Here, we determined GSH levels during the HIV-1 replication cycle. We observed a decline in GSH levels at all stages of infection (Fig. 1C, left panel). This decline was accompanied by an increase in GSSG levels at the early stage (12 h) followed by a decline at the later stage (24 h) compared to non-infected cells (Fig. 1C, middle panel). To predict the intracellular redox potential of this model, we calculated the ratio between GSH and GSSG. Results suggest an oxidizing environment in infected cells, which was particularly evident after 12 h of viral infection (Fig. 1C, right panel).

SOD1 serves as a redox biomarker and is present in the cytoplasm of host cells [45]. We observed an increase in SOD1 enzymatic activity in infected cells when compared to non-infected cells (Fig. 1D). However, SOD1 expression levels were reduced after 12 h of infection, compared to its expression at 2 h (Fig. 1E). Notably, we observed an increase in SOD1 expression levels in infected cells 24 h post-infection (Fig. 1E).

Enzymatic activity of GPx was investigated in infected $CD4^+$T cells and was increased at all stages (Fig. 1F). GR is required to maintain GSH in its reduced form and possibly to control the redox state of NADP in tissues where GSSG is available.

GR activity was elevated at the early (2 h) and late (24 and 36 h) stages of infection (Fig. 1G).

3.2. Endogenous and exogenous NO modulates the viral replication cycle

Upon HIV-1 infection, endogenous NO production showed the opposite trend compared to ROS generation (Fig. 1B), with NO levels increasing at 24 h ($p < 0.001$) and decreasing at 2, 12 and 36 h (Fig. 2A). Exposure of $CD4^+$T lymphocytes to increasing concentrations (0.1, 0.15 and 0.2 mM) of the NO donor SNAP was not toxic to these cells (Fig. 2B). Intracellular concentrations of nitrosated species and NO (NOx) after exposure to SNAP were 3.95 and 5.85 fluorescence (mean fluorescence intensity) in cells incubated respectively with 0.1 and 0.2 mM SNAP (Fig. 2C).Pre-incubation of the cells with the NO scavenger cPTIO (30 μM) reduced NO concentrations by half (Fig. 2C).

Jiménez et al. [46] showed that two NO donors, SNAP and SNP at low to moderate concentrations, stimulated HIV-1 infection of the human T-cell lines Jurkat and MT-2. We analyzed the effectiveness of infection based on viral load and the number of integrated HIV copies in HIV infected $CD4^+$T lymphocytes exposed or not exposed to 0.2 mM SNAP. In the absence of SNAP, we determined 4.7 copies/10^6 cells at 24 h, 4.8 copies/10^6 cells at 36 h and 2.3 copies/10^6 cells at 72 h (Fig. 2D). In contrast, exposure of cells to SNAP promoted an approximate 2.4-fold increase in the number of viral DNA copies after 72 h (Fig. 2D). The viral load was significantly increased relative to untreated infected cells (1.25 fold at 24 h, 1.18 fold at 36 h and 7.88 fold at 72 h) (Fig. 2E). These observations indicate that NO plays an important role in viral replication, increasing both the number of integrated HIV viral particles and viral load.

We evaluated whether the increase in viral load was dependent on NO levels. Differences in viral loads between SNAP treated, SNAP + cPTIO treated, and untreated infected cells at 72 h were used to build a geometric progression. After 18 days of infection, geometric progression calculations revealed that cells treated with SNAP would have 2×10^4 viral genomes in their supernatants while untreated cells or cells treated with SNAP + cPTIO would have no detectable viral genomes (Fig. 2F).

3.3. SNAP modulates the host's antioxidant defenses during the viral replication cycle

When infected cells were exposed to SNAP, at different periods post-infection (2, 12 and 36 h), SOD1 expression levels were higher than those determined in non-infected cells at the same time points (Fig. 3A). However, this increased expression was not followed by an increase in enzyme activity (Fig. 3B). As shown in Fig. 3C, SNAP stimulation promoted SOD1 nitration only in infected cells with increases at 24 and 36 h. Peroxynitrite oxidizes cysteine and tyrosine residues of SOD1 inhibiting enzyme activity [47,48].

We assessed the activity of GPx, a selenium-dependent enzyme, which is able to reduce H_2O_2 to H_2O and other peroxides with the oxidation of GSH [49]. The enzymatic activity of GPx was investigated in infected $CD4^+$ T cells and was increased at all stages, primarily after 2 h of infection (Fig. 3D). GR is another enzyme that is required to maintain GSH in its reduced form and possibly to control the redox state of NADP in tissues where GSSG is available [35]. GR activity was elevated at the early (2 h) and late (24 and 36 h) stages of infection (Fig. 3E).

Following the addition of SNAP, we observed an overall reduction in GR activity, when compared to controls without SNAP, at all stages of infection (Fig. 3E). Thus, SNAP showed a strong inhibitory effect on the primary enzymatic regulators of the cellular redox environment.

HIV infection induced a further decrease in GSH levels (Fig. 3F, left). Under these conditions, the ratio of GSH/GSSG was higher in cells treated only with the NO donor (Fig. 3F, right).

3.4. SNAP modulates the phosphorylation levels of PKC, Src and Akt in HIV-1 infected lymphocytes

It was previously shown that changes in the intracellular redox environment modulate PKC [50–53]. In addition, PKC phosphorylation can be induced by fusion of peptides with the enveloped HIV-1 virus [54,55]. We investigated the activation of PKC in HIV-1-infected $CD4^+$ T lymphocytes treated or not treated with SNAP. Pre-treatment of HIV-1-infected $CD4^+$T lymphocytes in the absence of SNAP with GF109203X (inhibitor of classical PKCs) promoted a decrease of 94% in viral load (Fig. 4A). GF109203X promoted a decrease of 90% in viral load of SNAP treated cells (Fig. 4A). These observations suggest that PKC activation by an exogenous source of NO is of major importance for HIV-1 replication.

Src kinase plays an important role in HIV infection and viral replication [56–60]. Src tyrosine kinases are essential for the activation of $CD4^+$ T cells and their inhibition can prevent the formation of HIV-1 reservoirs [61]. To determine if PKC and Src kinase constitute a signaling axis operative during HIV-1 infection in the presence or absence of SNAP treatment, we pre-treated isolated $CD4^+$T lymphocytes with GF109203X. The phosphorylation levels of Src kinase (Tyr416) were evaluated in cells treated or not treated with SNAP at 12 h post infection. In infected cells treated with SNAP we observed a decrease in Src kinase phosphorylation levels upon treatment with GF109203X (Fig. 4B).

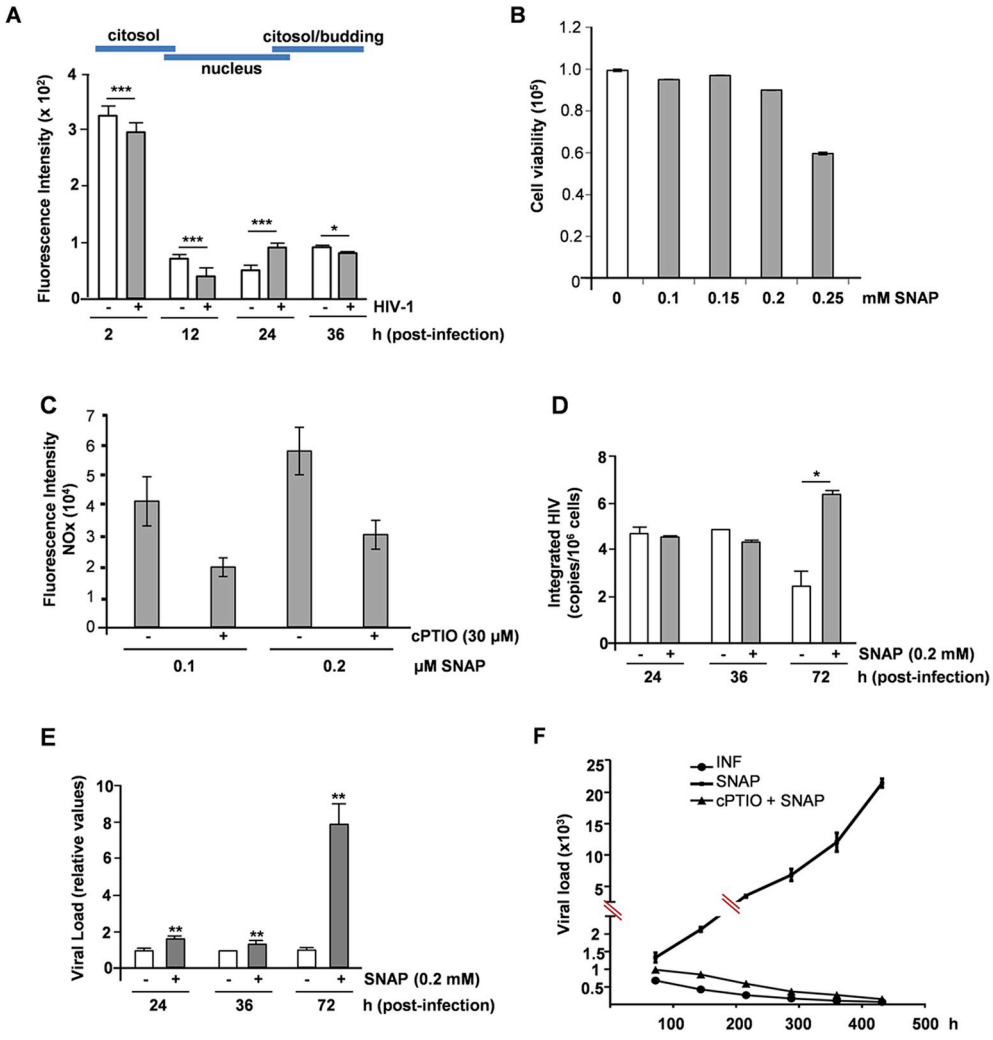

Fig. 2. Participation of nitric oxide in modulating HIV-1 infection in CD4$^+$ T lymphocytes. (**A**) Cells were seeded into twenty-four-well plates and infected with HIV-1. NO production was analyzed at different time points post-infection. This analysis was performed by incubating the cells with DAF-2 DA for 30 min prior to measuring intracellular NO production by infected and non-infected CD4$^+$ T lymphocytes on a flow cytometer. The schematic at the top of graph (**A**) indicates the three different stages of viral infection according to Mohammadi et al. (41): in the cytoplasm - early stage (2 h); nuclear integration - middle stage (12 h) and cytoplasm/budding - late stage (24 and 36 h). (**B**) CD4+T lymphocytes were cultivated in a 12-well culture plate and incubated with 0.1, 0.15, 0.2 and 0.25 mM of SNAP during 36 h at 37 °C. Cell viability was evaluated by trypan blue staining. (**C**) NO (NOx) release after SNAP treatment of CD4+T lymphocytes. Cells were incubated with 0.1 and 0.2 mM SNAP in the presence or absence of 30 µM cPTIO. Fluorescence intensities were normalized based on the number of cells per sample. (**D**) The number of virus copies integrated in CD4$^+$ T lymphocyte DNA with or without SNAP treatment was determined by qRT-PCR; no amplification was verified in non-infected cells. (**E**) Ratio of the increase in viral load after SNAP treatment in relation to untreated infected cells. (**F**) HIV-1 infection geometric progression based on differences in viral loads between SNAP treated, SNAP plus cPTIO-treated (30 µM) and untreated infected cells. Values were obtained by three independent experiments and are represented by the mean ± SD. All of the data shown in this figure were analyzed using Student's t-test for statistical comparisons (*$p < 0.05$, **$p < 0.01$, ***$p < 0.001$ and ****$p < 0.0001$). (For interpretation of the references to colour in this figure legend, the reader is referred to the Web version of this article.)

We then assayed the temporal modulation of PKC, Src kinase and Akt in infected cells treated or not treated with SNAP. Thus, we observed an increase in PKC phosphorylation at 2 and 24 h and a decrease at 12 and 36 h in infected cells (Fig. 4C, upper panel). Moreover, we observed differences in the phosphorylation levels of PKC after treatment with SNAP. We found increased phosphorylation levels at 2, 12 and 36 h and a decrease at 24 h post-infection in comparison to the phosphorylation levels determined for uninfected cells (Fig. 4D, upper panel). After 2 h, infected cells exhibited increased phosphorylation levels at Tyr416 of Src kinase, followed by a decrease at 12 and 36 h. Phosphorylation levels of Src kinase went up again at 24 h (Fig. 4C, middle panel). Interestingly, the Src phosphorylation profile was similar to the profile observed for PKC in cells treated with SNAP (Fig. 4D, middle panel). However, in infected cells not treated with SNAP, stimulation of Akt phosphorylation occurred only after 12 h of infection (Fig. 4C, lower panel), which was roughly the time point corresponding to the initiation of viral DNA integration [62]. Inhibition of Akt phosphorylation was detected at late stages of viral infection (24 and 36 h) (Fig. 4C, lower panel).

After SNAP treatment, a distinct Akt activation profile was observed. The infected cells showed an increase in Akt phosphorylation levels at 2, 12 and 36 h, whereas no activation was observed at the 24 h time point (Fig. 4D, lower panel). These observations strongly suggest that the stimulation of a host's signaling axis involving PKC, Src kinase and Akt by an exogenous source of NO is of major importance for HIV-1 replication.

4. Discussion

In the present study, we demonstrated that ROS generation, NO production, antioxidant enzyme activities, cellular signaling pathways and viral replication rates are influenced by the intracellular redox status during HIV-1 infection of human CD4$^+$T lymphocytes. Exposure of these cells to moderate concentrations of SNAP activated HIV-1 replication. The concentration of SNAP used in our study was very important, since higher concentrations promoted loss of cell viability.

The role of NO in HIV infection is still controversial. Some studies show that during HIV-1 infection there is a decrease in endogenous NO production, which may favor disease progression through the loss of NO-mediated antiviral and pro-apoptotic activities [26,63,64]. Decreased NO levels and inhibition of iNOS-related mRNA production have been detected in PBMCs from HIV-infected patients [28]. On the other hand, other studies report that NO production is increased in HIV patients [65–67]. Although these findings are conflicting, these studies do not take into account the effects of extracellular NO levels or the levels of NO produced by decomposition in the circulation of naturally occurring *S*-nitrosothiols [68,69].

Here, we show that in HIV-infected CD4$^+$T lymphocytes there is an increase in ROS generation and a decrease in endogenous NO production as compared to non-infected cells. This was evident in the early (at 2 h) and late stages (at 36 h) of the viral replication cycle. Changes in the intracellular redox environment associated with HIV-1 infection

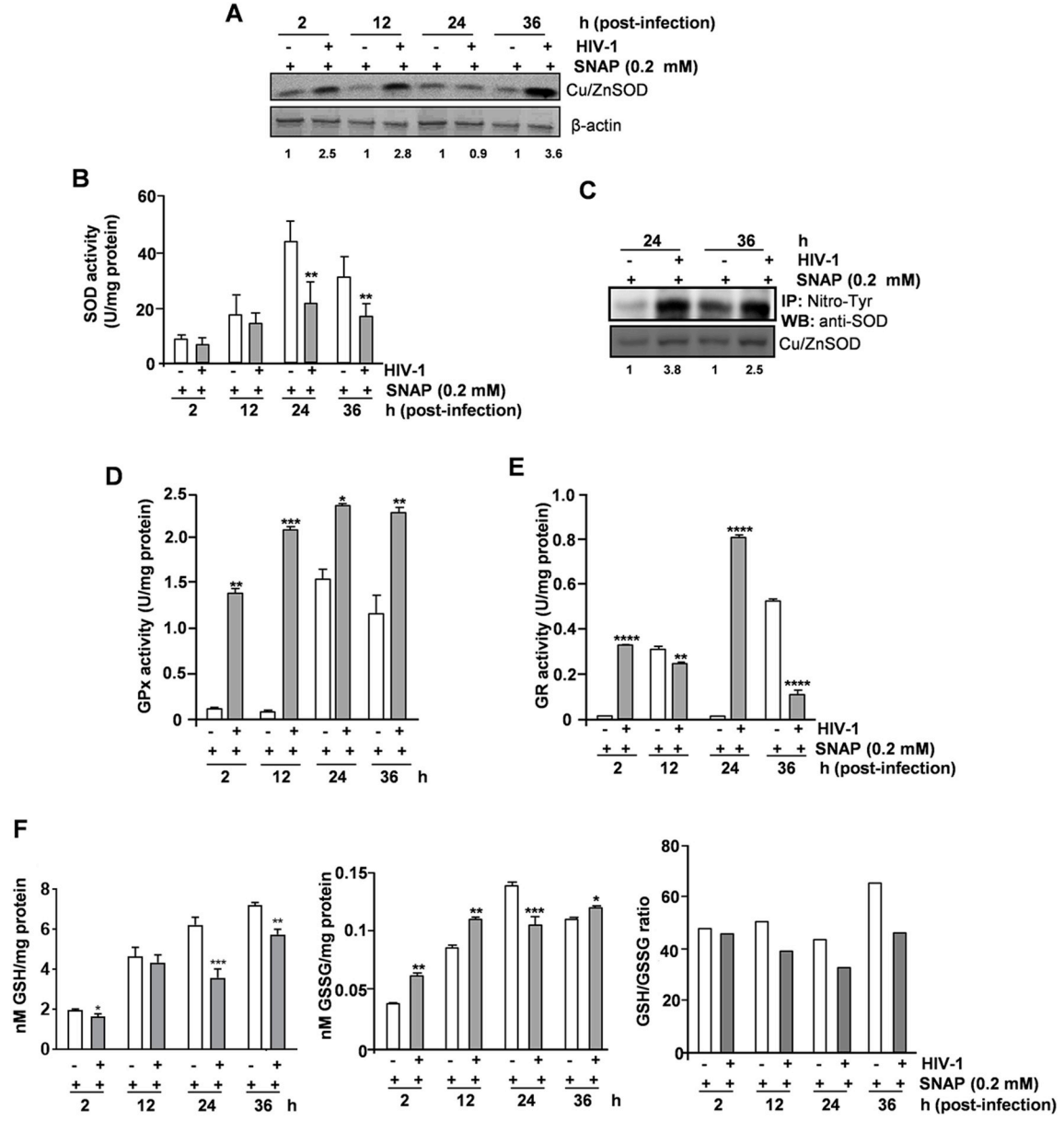

Fig. 3. Antioxidant enzyme activity profile during HIV-1 infection. (**A**) Analyses of Cu/ZnSOD expression in infected and non-infected CD4$^+$ T lymphocytes treated with SNAP were assayed by Western blots probed with a mouse monoclonal anti-Cu/ZnSOD. The values below the images correspond to the relative measurements obtained. The Western blot is representative for three independent experiments. (**B**) A Cu/ZnSOD enzymatic activity assay was performed at different time points after HIV-1 infection of CD4$^+$ T lymphocytes treated with SNAP. Sidak's multiple comparisons test was used for statistical comparisons, and the observed differences were statistically significant. Error bars represent three independent experiments and are represented by the mean ± SD (**$p < 0.01$ and ***$p < 0.001$). (**C**) Nitrated Cu/ZnSOD profile of infected and non-infected CD4$^+$ T lymphocytes treated with SNAP at 24 and 36 h post-infection. The profile was obtained by an immunoprecipitation assay (immunoprecipitation with Nitro-Tyr antibody, detection of Cu/ZnSOD using anti-SOD antibody). The Western blot is representative for three independent experiments. The enzymatic activity assay was performed at different time points after HIV-1 infection of CD4$^+$ T lymphocytes. GPx (**D**) or GR (**E**) enzymatic activity was assessed in infected and non-infected CD4$^+$ T cells and in cells treated with SNAP. The quantifications are for different time points after CD4 + T lymphocyte infection. (**F**) Quantification of GSH (left), GSSG (middle) and the GSH/GSSG ratio (right panel) in infected and non-infected CD4$^+$ T lymphocytes treated with SNAP (0.2 mM). The GSH/GSSG ratios (right panel) are the GSH levels divided by the GSSG levels. Student's t-test was used for statistical comparisons, and the observed differences were statistically significant (*$p < 0.05$; **$p < 0.01$; ***$p < 0.001$). Error bars represent ± SD of n = 3.

could be translated into enzymatic and non-enzymatic antioxidant related activities. Upon HIV-1 infection, SOD1 expression levels and activity increased during the early and late stages of the infection cycle, which correspond to viral entry and viral transit through the cytoplasm of the host cell to HIV-1 budding, respectively [37]. In addition, HIV-1 infection stimulated GPx activity in CD4$^+$T lymphocytes at all stages of the process. Accordingly, GR activity was elevated in infected cells during the initial period of HIV-1 infection. Therefore, during this early phase of infection, oxidative stress conditions determine the dynamics of the process, in which viral replication proceeds at decreasing rates.

However, exposure of HIV-infected CD4$^+$T lymphocytes to SNAP resulted in strong stimulation of viral replication in these cells. These findings can be rationalized by assuming that upon addition of an exogenous source of NO, nitrative and nitrosative stress conditions take place in the intracellular environment. In the aqueous phase the reaction of NO with $O_2^{\cdot-}$ is very efficient and generates $ONOO^-$ which rapidly reacts with carbon dioxide leading to the formation of $CO_3^{\cdot-}$ and $\cdot NO_2$ [70]. Increased nitration of SOD1 is indirect evidence of $ONOO^-$

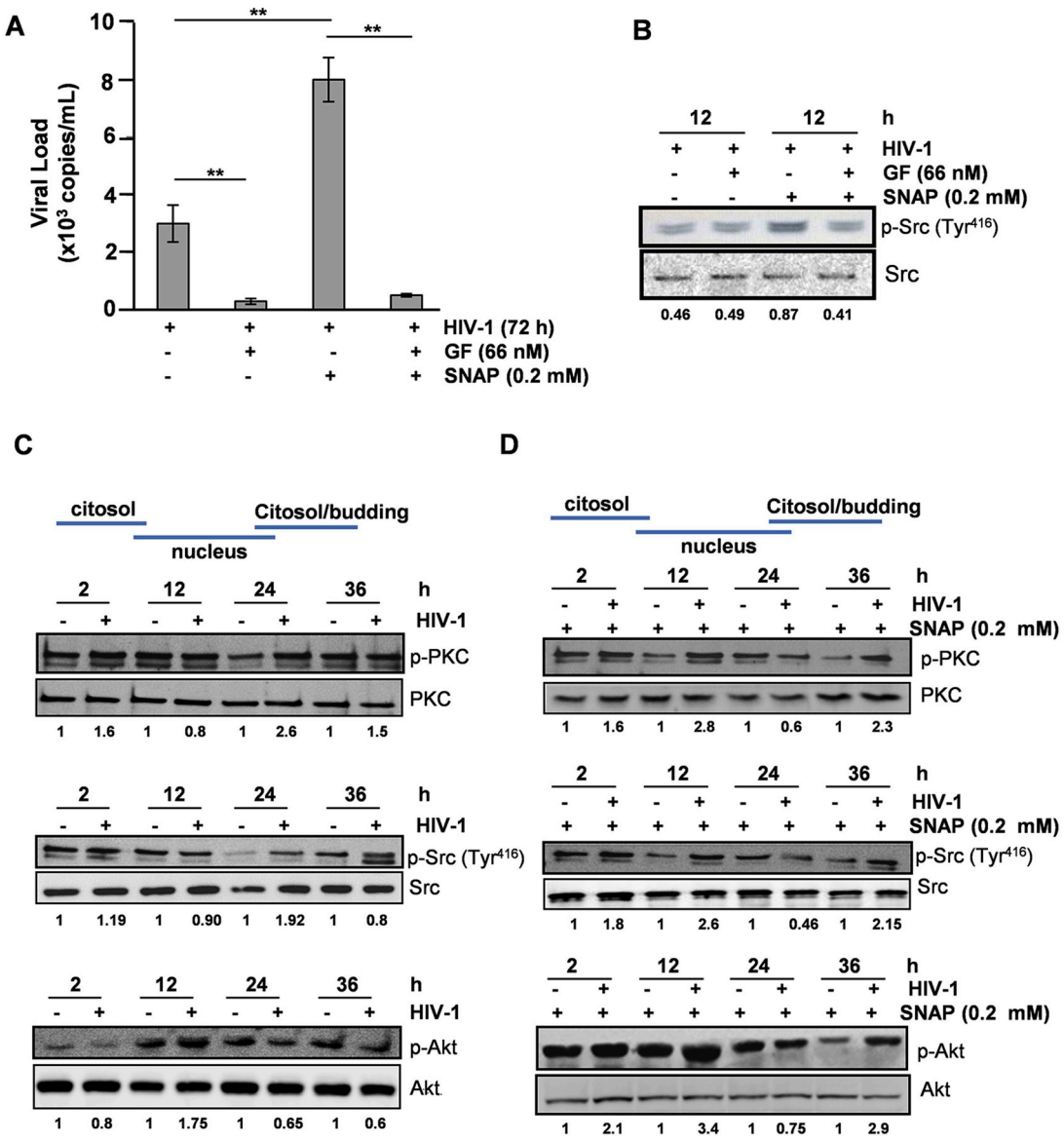

Fig. 4. PKC, Src kinase and Akt phosphorylation profiles during HIV-1 infection. (**A**) $CD4^+$ T lymphocytes infected and not infected with HIV-1 were cultured with or without 66 nM GF109203X (a PKC inhibitor) for 60 min followed by treatment with 0.2 mM SNAP at 37 °C. Ratio showing the increase in viral load after SNAP treatment in relation to untreated infected cells. Values were obtained by three independent experiments and are represented by the mean ± SD. Student's t-test was used for statistical comparisons, and the observed differences were statistically significant (**$p < 0.01$). (**B**) Analysis of Src activation in infected $CD4^+$ T lymphocytes treated with SNAP, in the presence or absence of GF109203X (66 nM), assayed by Western blots probed with a mouse monoclonal anti-Src (phosphoTyr416). $CD4^+$ T lymphocytes infected and not infected with HIV-1 without (**C**) or with 0.2 mM SNAP (**D**) at 37 °C. The cells were lysed, and total protein lysates were immunoblotted with anti-phospho PKC or anti-PKC (upper panel), anti-phospho-Src-(Tyr416) or anti-Src (middle panel) and anti-phospho Akt or anti-Akt (lower panel) antibodies. The values below the images correspond to the relative measurements obtained. The Western blots are representative for three independent experiments.

formation and is associated with decreased enzyme activity, as shown by MacMillan-Crow et al. [71]. Decreases in activity of the antioxidant enzymes GPx and GR and alterations in the GSH/GSSG ratio may also be associated with $ONOO^-$ formation [72–74].

SNAP reacts with GSH because of its vast excess over every other thiol in the cell cytoplasm. The equilibrium constants for transnitrosation between SNAP and GSH favor GSNO formation [31,75]. This could explain the low levels of GSH in cells treated with SNAP. In addition, in the presence of SNAP we observed a drastic decrease in GR activity, probably due to the inhibitory effect of *S*-nitrosylation of a critical cysteine residue important for enzyme activity [76].

Here we show that a signaling axis involving PKC, Src kinase and Akt is operative upon HIV-1 infection of $CD4^+$T lymphocytes. PKC phosphorylation levels increased at 2 and 24 h and decreased at 12 and 36 h post-infection. A decrease of PKC phosphorylation levels during the last stage of infection (36 h) may be temporally associated with the assembly and budding of viral particles [77].

Upon HIV-1 infection, Src kinase recruits Nef and triggers signals to PKC, Akt and SOD1 [62,75,77–79]. Accordingly, we observed increased SOD1 expression (24 h) and activity (2, 12, 24 and 36 h) that was accompanied by an increase in Src kinase activity. The constitutive activation of Src kinase or stable expression of Src kinase will concomitantly stimulate an increase in PKC-mediated signaling [80–84].

François and Klotman [85] showed the importance of the signaling pathway triggered by gp120 that involved PI3K with Akt as downstream targets. The three proteins played a crucial role in the initial

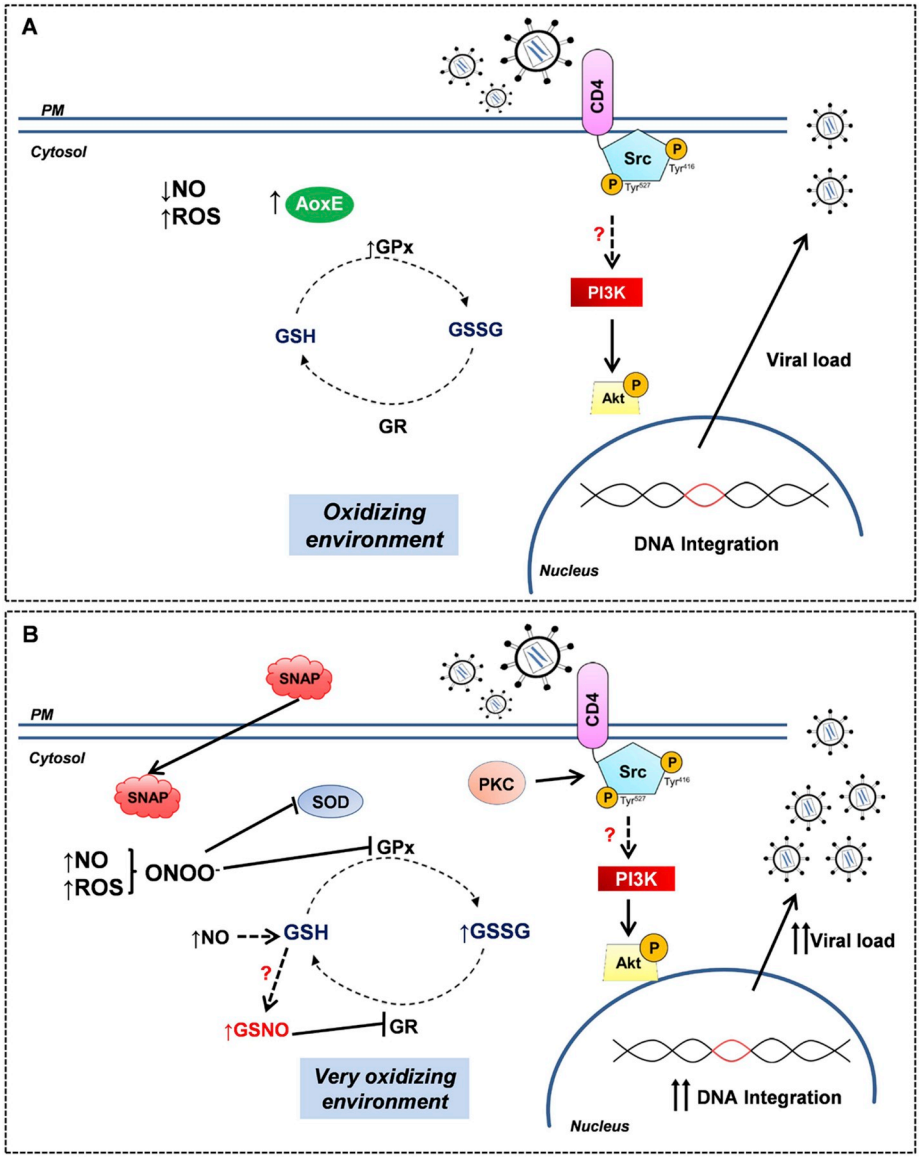

Fig. 5. General scheme of the HIV-1 infection signaling pathways associated with an intracellular redox environment. (**A**) During the early stage of the HIV-1 replicative cycle an increase in ROS production and a decrease in intracellular NO levels were observed. ROS induced phosphorylation of the Tyr416 Src residue with secondary Akt phosphorylation, which triggered an important pathway for the establishment of infection. ROS production in the late stage of infection led to the recruitment of antioxidant enzymes (AoxE) with a concomitantly progressive decline in GSH levels and an increase in GSSG levels, indicating an oxidizing environment. This modification activated Src through the phosphorylation of the Tyr416 residue and subsequent activation of PKC phosphorylation. (**B**) SNAP treatment possibly results in peroxynitrite ($ONOO^-$) generation. Alternatively, the NO donor induces PKC phosphorylation leading to Src activation. Furthermore, although SNAP induced Cu/ZnSOD nitration, an increase was not observed in its activity. The manipulation of the redox environment promoted Akt phosphorylation during the early and late stages of infection to trigger the establishment of infection and cell survival, respectively. The antioxidant enzymes GR and GPx were recruited to neutralize ROS with a progressive decline in the GSH level and an increase in the GSSG level, indicating an oxidizing environment. These alterations promoted by SNAP treatment resulted in an increase in viral DNA integration and viral load.

steps of HIV-1 infection prior to integration [85]. Recent studies have shown that Akt activation is especially triggered by Nef protein in T cells or MDMs cells treated with exogenous Nef. After the use of protease inhibitors (PIs), which present immunomodulatory effects by blocking or decreasing Akt activation, HIV-1 reservoirs were decreased. This result shows the important evidence for therapeutic use of HIV-1 PI in order to decrease latently infected cells in HIV-1-infected patients [86,87]. We observed the activation of Akt at 12 h, which approximately corresponded to the moment of reverse transcription completion and integration. The Akt activation profile (after 12 h of infection) was different from the profile observed for the other proteins described herein.

Addition of SNAP to the infected cultures promoted posttranslational modifications on proteins belonging to the signaling axis discussed above.

A decrease in intracellular NO levels upon HIV-1 infection could be compensated by exogenously added SNAP. Exogenous NO could provide cytoprotection against the oxidative stress conditions generated by HIV-1 infection through PKC activation. Early studies corroborate our assumption by establishing a connection between NO-mediated activation of PKC and downstream activation of NF-E2-related factor 2 (Nrf2) [88].

Nrf2 is one of the transcription factors that provide cellular protection against oxidative stress [89]. PKC phosphorylation exhibited a similar profile compared to the Src kinase profile before and after SNAP treatment, presenting an increase at 12 h and 36 h and a decrease at 24 h. Alternatively, SNAP can directly activate Src through a mechanism independent of dephosphorylation of phospho-Tyr527[31]. The phosphorylation profiles exhibited by PKC and Src kinase in the presence or absence of SNAP treatment, suggest the existence of a signaling axis connecting these two proteins.

SNAP treatment led to early (2 h) and late (36 h) phosphorylation of Akt. In the absence of SNAP treatment, Akt phosphorylation was observed only after 12 h of infection. The association between the activation of the host's kinases PKC, Src kinase and Akt and the pro-oxidant environment created by HIV infection in the presence or absence of SNAP promotes conditions for the survival and growth of the virus.

As mentioned above, we detected Akt phosphorylation in cells at the time post infection corresponding to viral DNA integration. It is known that the immediate downstream target of Akt is the protein kinase mammalian target of rapamycin (mTOR). Specifically, the catalytic subunit complex mTORC2 regulates cell survival and cytoskeletal organization with the participation of Akt and protein kinase C alpha (PKCα), respectively [90]. When rapamycin (RAPA) was tested in HIV-

infected SCID mice reconstituted with human peripheral blood leucocytes, RAPA inhibited HIV replication preventing a decrease in CD4 cells, thereby preserving the original CD4: CD8 cell ratio [91]. Treatment with RAPA decreased provirus formation and reduced HIV-RNA [90,92]. Protease inhibitors and RAPA interfere with HIV replication by targeting Akt and mTOR, respectively, indicating a possible anti-viral role.

We showed an increase in Akt phosphorylation after SNAP treatment. It was previously shown in human melanoma cells that NO can potentially induce the mTOR pathway by acting either on or upstream of Akt [93]. Immunohistochemical analysis of tumor specimens from stage III melanoma showed a significant correlation between iNOS expression and the mTOR pathway. Exogenously supplied NO (DEA-NONOate) could reverse mTOR inhibition by the B-Raf inhibitor vemurafenib [93].

Following the addition of SNAP, we observed an increase in viral load with a pronounced peak at 72 h post-infection representing an approximately 8.0-fold increase (Fig. 2E). Therefore, we can infer that SNAP treatment in HIV-infected $CD4^+$ T lymphocytes increases viral DNA content and viral load, which may be directly related to increased virus production in the activated cells. SNAP treatment also increased the viral load after 72 h in infected cells pre-treated with GF109203X (Fig. 4D). These observations are very interesting because viral load fluctuations are related to clinically relevant outcomes. Variations in viral load as high as 0.5 log present a significant clinical impact on disease progression and on the therapeutic response to antiretroviral treatments [94,95]. In previous studies, an association was shown between high viral load and increased NO production in the serum of HIV-infected symptomatic and asymptomatic patients [96–98]. Accumulation of NO metabolites was observed in patients with central nervous system complications [98]. In this condition, there is a derangement of immune system functions associated with increased NO levels.

The use of highly active anti-retroviral therapy (HAART) promotes a decline in the levels of NO metabolites and this situation potentially contributes towards cardiovascular disease in HIV-infected patients [66].

To avoid the increases in viral load or the development of viral resistance, as well as higher cardiovascular and atherosclerosis risk, the use of NO supplementation is advisable only in HIV patients on HAART treatment.

5. Conclusions

In conclusion, during the HIV-1 replication cycle, we observed an increase in ROS production and a decrease in intracellular NO levels. During the early stage of infection, ROS induced phosphorylation and activation of PKC and Src kinase, and promoted Akt phosphorylation, thereby triggering an important pathway to establish infection. The increases in ROS production led to activation of the antioxidant enzymes SOD1, GPx and GR. At the same time, we observed a progressive decline in GSH levels, accompanied by an increase in the GSSG level, indicating an oxidizing environment. In this scenario, SNAP treatment potentially promotes $ONOO^-$ and/or GSNO generation. SNAP-derived changes of the redox environment promoted PKC, Src kinase and Akt activation during the early and late stages of infection.

These alterations promoted by SNAP treatment resulted in an increase in viral DNA integration and viral load. Our findings are summarized in Fig. 5.

Funding

This work was supported by grants from Fundação de Amparo à Pesquisa do Estado de São Paulo (FAPESP, 2010/07236-1 and 2010/09366-0).

Acknowledgments

We thank Dr. Giovana A. Gonçalves for the flow cytometer support, MSc James Daltro for help with figures, the Retrovirology and Viral Load Laboratories from Hospital São Paulo for the technical support regarding viral load quantification and the Charitable Association of Blood Collection (COLSAN) for the support and donation of blood bags.

References

[1] D. Emilie, et al., Cytokines in HIV infection, Int. J. Immunopharmacol. (1994), https://doi.org/10.1016/0192-0561(94)90026-4.
[2] N. Israël, M.A. Gougerot-Pocidalo, Oxidative stress in human immunodeficiency virus infection, Cell. Mol. Life Sci. 53 (1997) 864–870.
[3] H.P. Eck, et al., Low concentrations of acid-soluble thiol (cysteine) in the blood plasma of HIV-1-infected patients, Biol. Chem. Hoppe Seyler 370 (1989) 101–108.
[4] F.J. Staal, et al., Intracellular glutathione levels in T cell subsets decrease in HIV-infected individuals, AIDS Res. Hum. Retrovir. 8 (1992) 305–311.
[5] H. Masutani, et al., Dysregulation of adult T-cell leukemia-derived factor (ADF)/thioredoxin in HIV infection: loss of ADF high-producer cells in lymphoid tissues of AIDS patients, AIDS Res. Hum. Retrovir. 8 (1992) 1707–1715.
[6] H. Nakamura, et al., Elevation of plasma thioredoxin levels in HIV-infected individuals, Int. Immunol. 8 (1996) 603–611.
[7] E. Peterhans, Reactive oxygen species and nitric oxide in viral diseases, Biol. Trace Elem. Res. 56 (1997) 107–116.
[8] J.P. Allard, et al., Effects of vitamin E and C supplementation on oxidative stress and viral load in HIV-infected subjects, AIDS 12 (1998) 1653–1659.
[9] R. Lee, P. Beauparlant, H. Elford, P. Ponka, J. Hiscott, Selective inhibition of l kappaB alpha phosphorylation and HIV-1 LTR-directed gene expression by novel antioxidant compounds, Virology 234 (1997) 277–290.
[10] A. Mandas, et al., Oxidative imbalance in HIV-1 infected patients treated with antiretroviral therapy, J. Biomed. Biotechnol. 2009 (2009) 749575.
[11] J.A. Martin, J. Sastre, J.G. de la Asunción, F.V. Pallardó, J. Viña, Hepatic gamma-cystathionase deficiency in patients with AIDS, J. Am. Med. Assoc. 285 (2001) 1444–1445.
[12] I.I. Kruman, A. Nath, M.P. Mattson, HIV-1 protein Tat induces apoptosis of hippocampal neurons by a mechanism involving caspase activation, calcium overload, and oxidative stress, Exp. Neurol. 154 (1998) 276–288.
[13] H.-C. Yang, et al., Small-molecule screening using a human primary cell model of HIV latency identifies compounds that reverse latency without cellular activation, J. Clin. Investig. 119 (2009) 3473–3486.
[14] S. Mihm, J. Ennen, U. Pessara, R. Kurth, W. Dröge, Inhibition of HIV-1 replication and NF-kappa B activity by cysteine and cysteine derivatives, AIDS 5 (1991) 497–503.
[15] G. Nabel, D. Baltimore, An inducible transcription factor activates expression of human immunodeficiency virus in T cells, Nature 326 (1987) 711–713.
[16] R. Schreck, P. Rieber, P.A. Baeuerle, Reactive oxygen intermediates as apparently widely used messengers in the activation of the NF-kappa B transcription factor and HIV-1, EMBO J. 10 (1991) 2247–2258.
[17] M.O. Westendorp, et al., HIV-1 Tat potentiates TNF-induced NF-kappa B activation and cytotoxicity by altering the cellular redox state, EMBO J. 14 (1995) 546–554.
[18] C. Bogdan, C. Bogdan, Nitric oxide and the immune response, Nat. Immunol. 2 (2001) 907–916.
[19] Mannick, J. B. The antiviral role of nitric oxide. Res. Immunol. 146, 693–697.
[20] K.A. Krogh, N. Wydeven, K. Wickman, S.A. Thayer, HIV-1 protein Tat produces biphasic changes in NMDA-evoked increases in intracellular Ca^{2+} concentration via activation of Src kinase and nitric oxide signaling pathways, J. Neurochem. 130 (2014) 642–656.
[21] J.B. Mannick, et al., Nitric oxide modulates HIV-1 replication, J. Acquir. Immune Defic. Syndr. 22 (1999) 1–9.
[22] J.S. Beckman, W.H. Koppenol, Nitric oxide, superoxide, and peroxynitrite: the good, the bad, and ugly, Am. J. Physiol. Physiol. 271 (1996) C1424–C1437.
[23] C. Brito, et al., Peroxynitrite inhibits T lymphocyte activation and proliferation by promoting impairment of tyrosine phosphorylation and peroxynitrite-driven apoptotic death, J. Immunol. 162 (1999) 3356–3366.
[24] R. Radi, G. Peluffo, M.N. Alvarez, M. Naviliat, A. Cayota, Unraveling peroxynitrite formation in biological systems, Free Radic. Biol. Med. 30 (2001) 463–488.
[25] L. Uzasci, M.A. Bianchet, R.J. Cotter, A. Nath, Identification of nitrated immunoglobulin variable regions in the HIV-infected human brain: implications in HIV infection and immune response, J. Proteome Res. 13 (2014) 1614–1623.
[26] E. Cairoli, D. Scott-Algara, O. Pritsch, G. Dighiero, A. Cayota, HIV-1 induced decrease of nitric oxide production and inducible nitric oxide synthase expression during in vivo and in vitro infection, Clin. Immunol. 127 (2008) 26–33.
[27] Lander Cellular, Activation mediated by nitric oxide, Methods 10 (1996) 15–20.
[28] H.M. Lander, et al., Redox regulation of cell signalling, Nature 381 (1996) 380–381.
[29] H.M. Lander, D.M. Levine, A. Novogrodsky, Haemin enhancement of glucose transport in human lymphocytes: stimulation of protein tyrosine phosphatase and activation of p56lck tyrosine kinase, Biochem. J. 291 (1993) 281–287 (Pt 1).
[30] H.M. Lander, P. Sehajpal, D.M. Levine, A. Novogrodsky, Activation of human peripheral blood mononuclear cells by nitric oxide-generating compounds, J. Immunol. 150 (1993) 1509–1516.
[31] M.F. Curcio, et al., Regulatory effects of nitric oxide on Src kinase, FAK, p130Cas, and receptor protein tyrosine phosphatase alpha (PTP-alpha): a role for the cellular

redox environment, Antioxidants Redox Signal. 13 (2010) 109–125.
[32] T. Nagano, Practical methods for detection of nitric oxide, Luminescence 14 (1999) 283–290.
[33] I. Rahman, A. Kode, S. Biswas, Assay for quantitative determination of glutathione and glutathione disulfide levels using enzymatic recycling method, Nat. Protoc. 1 (2006) 3159–3165.
[34] R. Brigelius-Flohé, Glutathione peroxidases and redox-regulated transcription factors, Biol. Chem. 387 (2006) 1329–1335.
[35] I. Carlberg, B. Mannervik, Purification and characterization of the flavoenzyme glutathione reductase from rat liver, J. Biol. Chem. 250 (1975) 5475–5480.
[36] J.F. Ewing, D.R. Janero, Microplate superoxide dismutase assay employing a nonenzymatic superoxide generator, Anal. Biochem. 232 (1995) 243–248.
[37] P. Mohammadi, et al., 24 hours in the life of HIV-1 in a T cell line, PLoS Pathog. 9 (2013) e1003161.
[38] S.V. Komninakis, et al., HIV-1 proviral DNA loads (as determined by quantitative PCR) in patients subjected to structured treatment interruption after antiretroviral therapy failure, J. Clin. Microbiol. 50 (2012) 2132–2133.
[39] A.N. Colado Simão, V.J. Victorino, H.K. Morimoto, E.M.V. Reiche, C. Panis, Redox-driven events in the human immunodeficiency virus type 1 (HIV-1) infection and their clinical implications, Curr. HIV Res. 13 (2015) 143–150.
[40] E.W. Taylor, et al., Nutrition, HIV, and drug abuse: the molecular basis of a unique role for selenium, J. Acquir. Immune Defic. Syndr. 25 (Suppl 1) (2000) S53–S61.
[41] L. Zhao, B. Olubajo, E.W. Taylor, Functional studies of an HIV-1 encoded glutathione peroxidase, Biofactors 27 (2006) 93–107.
[42] H.Y. Song, et al., Topical transduction of superoxide dismutase mediated by HIV-1 Tat protein transduction domain ameliorates 12-O-tetradecanoylphorbol-13-acetate (TPA)-induced inflammation in mice, Biochem. Pharmacol. 75 (2008) 1348–1357.
[43] L. Gil, et al., Contribution to characterization of oxidative stress in HIV/AIDS patients, Pharmacol. Res. 47 (2003) 217–224.
[44] J. Lu, A. Holmgren, The thioredoxin antioxidant system, Free Radic. Biol. Med. 66 (2014) 75–87.
[45] J. Kärkkäinen, T. Selander, M. Purdy, P. Juvonen, M. Eskelinen, Patients with increased levels of the oxidative stress biomarker SOD1 appear to have diminished postoperative pain after midline laparotomy: a randomised trial with special reference to postoperative pain score (NRS), Anticancer Res. 38 (2018) 1003–1008.
[46] J.L. Jimenez, J. Gonzalez-Nicolas, S. Alvarez, M. Fresno, M.A. Munoz-Fernandez, Regulation of human immunodeficiency virus type 1 replication in human T lymphocytes by nitric oxide, J. Virol. 75 (2001) 4655–4663.
[47] C. Quijano, et al., Reaction of peroxynitrite with Mn-superoxide dismutase. Role of the metal center in decomposition kinetics and nitration, J. Biol. Chem. 276 (2001) 11631–11638.
[48] C. Quijano, B. Alvarez, R.M. Gatti, O. Augusto, R. Radi, Pathways of peroxynitrite oxidation of thiol groups, Biochem. J. 322 (1997) 167–173 (Pt 1).
[49] R. Brigelius-Flohé, M. Maiorino, Glutathione peroxidases, Biochim. Biophys. Acta 1830 (2013) 3289–3303.
[50] Y.-S. Jung, et al., Role for PKC-epsilon in neuronal death induced by oxidative stress, Biochem. Biophys. Res. Commun. (2004), https://doi.org/10.1016/j.bbrc.2004.05.217.
[51] A.M.N. Kabir, et al., Cardioprotection initiated by reactive oxygen species is dependent on activation of PKCepsilon, Am. J. Physiol. Heart Circ. Physiol. (2006), https://doi.org/10.1152/ajpheart.00798.2005.
[52] M.E. Barnett, D.K. Madgwick, D.J. Takemoto, Protein kinase C as a stress sensor, Cell. Signal. (2007), https://doi.org/10.1016/j.cellsig.2007.05.014.
[53] R. Rathore, et al., Hypoxia activates NADPH oxidase to increase [ROS]i and [Ca2+]i through the mitochondrial ROS-PKCe{open} signaling axis in pulmonary artery smooth muscle cells, Free Radic. Biol. Med. (2008), https://doi.org/10.1016/j.freeradbiomed.2008.06.012.
[54] M. Vitiello, et al., Viral fusion peptides induce several signal transduction pathway activations that are essential for interleukin-10 and beta-interferon production, Intervirology 53 (2010) 381–389.
[55] C. Phetsouphanh, a D. Kelleher, The role of PKC-theta in CD4+ T cells and HIV infection: to the nucleus and back again, Front. Immunol. (2015), https://doi.org/10.3389/fimmu.2015.00391.
[56] C.H. Lee, et al., Crystal structure of the conserved core of HIV-1 Nef complexed with a Src family SH3 domain, Cell (1996), https://doi.org/10.1016/S0092-8674(00)81276-3.
[57] S. Grzesiek, et al., The solution structure of HIV-1 Nef reveals an unexpected fold and permits delineation of the binding surface for the SH3 domain of Hck tyrosine protein kinase, Nat. Struct. Biol. (1996), https://doi.org/10.1038/nsb0496-340.
[58] S. Arold, et al., The crystal structure of HIV-1 Nef protein bound to the Fyn kinase SH3 domain suggests a role for this complex in altered T cell receptor signaling, Structure (1997), https://doi.org/10.1016/S0969-2126(97)00286-4.
[59] X. Jia, et al., Structural basis of evasion of cellular adaptive immunity by HIV-1 Nef, Nat. Struct. Mol. Biol. (2012), https://doi.org/10.1038/nsmb.2328.
[60] X. Ren, S.Y. Park, J.S. Bonifacino, J.H. Hurley, How HIV-1 Nef hijacks the AP-2 clathrin adaptor to downregulate CD4, Elife (2014), https://doi.org/10.7554/eLife.01754.001.
[61] M. Coiras, J. Ambrosioni, F. Cervantes, J.M. Miró, J. Alcamí, Tyrosine kinase inhibitors: potential use and safety considerations in HIV-1 infection, Expert Opin. Drug Saf. (2017), https://doi.org/10.1080/14740338.2017.1313224.
[62] J.-J. Jeong, B. Kim, D.-H. Kim, Ginsenoside Rb1 eliminates HIV-1 (D3)-transduced cytoprotective human macrophages by inhibiting the AKT pathway, J. Med. Food 17 (2014) 849–854.
[63] C. Bogdan, Nitric oxide and the immune response, Nat. Immunol. 2 (2001) 907–916.
[64] G. Barbaro, et al., Intensity of myocardial expression of inducible nitric oxide synthase influences the clinical course of human immunodeficiency virus-associated cardiomyopathy. Gruppo Italiano per lo Studio Cardiologico dei pazienti affetti da AIDS (GISCA), Circulation 100 (1999) 933–939.
[65] R. Zangerle, et al., Serum nitrite plus nitrate in infection with human immunodeficiency virus type-1, Immunobiology 193 (1995) 59–70.
[66] R.M. Soccal, J.A.M. de Carvalho, G.V. Bochi, R.N. Moresco, J.E.P. da Silva, Nitric oxide levels in HIV-infected, untreated patients and HIV-infected patients receiving antiretroviral therapy, Biomed. Pharmacother. 79 (2016) 302–307.
[67] L. Gama, et al., Expansion of a subset of CD14highCD16negCCR2low/neg monocytes functionally similar to myeloid-derived suppressor cells during SIV and HIV infection, J. Leukoc. Biol. 91 (2012) 803–816.
[68] B. Guikema, Q. Lu, D. Jourd'heuil, Chemical considerations and biological selectivity of protein nitrosation: implications for NO-mediated signal transduction, Antioxidants Redox Signal. 7 (2005) 593–606.
[69] D. Torre, A. Pugliese, F. Speranza, Role of nitric oxide in HIV-1 infection: friend or foe? Lancet Infect. Dis. 2 (2002) 273–280.
[70] C. Szabó, H. Ischiropoulos, R. Radi, Peroxynitrite: biochemistry, pathophysiology and development of therapeutics, Nat. Rev. Drug Discov. 6 (2007) 662–680.
[71] L.A. MacMillan-Crow, J.P. Crow, J.D. Kerby, J.S. Beckman, J.A. Thompson, Nitration and inactivation of manganese superoxide dismutase in chronic rejection of human renal allografts, Proc. Natl. Acad. Sci. U. S. A 93 (1996) 11853–11858.
[72] D. Francescutti, J. Baldwin, L. Lee, B. Mutus, Peroxynitrite modification of glutathione reductase: modeling studies and kinetic evidence suggest the modification of tyrosines at the glutathione disulfide binding site, Protein Eng. 9 (1996) 189–194.
[73] S. Padmaja, G.L. Squadrito, W.A. Pryor, Inactivation of glutathione peroxidase by peroxynitrite, Arch. Biochem. Biophys. 349 (1998) 1–6.
[74] M. Trujillo, R. Radi, Peroxynitrite reaction with the reduced and the oxidized forms of lipoic acid: new insights into the reaction of peroxynitrite with thiols, Arch. Biochem. Biophys. 397 (2002) 91–98.
[75] E. Olivetta, et al., HIV-1 Nef induces p47(phox) phosphorylation leading to a rapid superoxide anion release from the U937 human monoblastic cell line, J. Cell. Biochem. 106 (2009) 812–822.
[76] S.P. Singh, J.S. Wishnok, M. Keshive, W.M. Deen, S.R. Tannenbaum, The chemistry of the S-nitrosoglutathione/glutathione system, Proc. Natl. Acad. Sci. U. S. A 93 (1996) 14428–14433.
[77] R.J. Juszczak, H. Turchin, A. Truneh, J. Culp, S. Kassis, Effect of human immunodeficiency virus gp120 glycoprotein on the association of the protein tyrosine kinase p56lck with CD4 in human T lymphocytes, J. Biol. Chem. 266 (1991) 11176–11183.
[78] A.B. Strasner, et al., The Src kinase Lck facilitates assembly of HIV-1 at the plasma membrane, J. Immunol. 181 (2008) 3706–3713.
[79] J.R. Bayascas, Dissecting the role of the 3-phosphoinositide-dependent protein kinase-1 (PDK1) signalling pathways, Cell Cycle 7 (2008) 2978–2982.
[80] J. Finley, Oocyte activation and latent HIV-1 reactivation: AMPK as a common mechanism of action linking the beginnings of life and the potential eradication of HIV-1, Med. Hypotheses 93 (2016) 34–47.
[81] S. Delage, et al., Increased protein kinase C alpha expression in human colonic Caco-2 cells after insertion of human Ha-ras or polyoma virus middle T oncogenes, Cancer Res. 53 (1993) 2762–2770.
[82] S.A. Qureshi, C.K. Joseph, M. Rim, A. Maroney, D.A. Foster, v-Src activates both protein kinase C-dependent and independent signaling pathways in murine fibroblasts, Oncogene 6 (1991) 995–999.
[83] Q. Zang, P. Frankel, D.A. Foster, Selective activation of protein kinase C isoforms by v-Src, Cell Growth Differ. 6 (1995) 1367–1373.
[84] G. Doyon, et al., Discovery of a small molecule agonist of phosphatidylinositol 3-kinase p110α that reactivates latent HIV-1, PLoS One 9 (2014) e84964.
[85] F. François, M.E. Klotman, Phosphatidylinositol 3-kinase regulates human immunodeficiency virus type 1 replication following viral entry in primary CD4+ T lymphocytes and macrophages, J. Virol. 77 (2003) 2539–2549.
[86] A. Kumar, et al., Tuning of AKT-pathway by Nef and its blockade by protease inhibitors results in limited recovery in latently HIV infected T-cell line, Sci. Rep. 6 (2016) 24090.
[87] S. Pasquereau, A. Kumar, W. Abbas, G. Herbein, Counteracting Akt activation by HIV protease inhibitors in monocytes/macrophages, Viruses 10 (2018) 190.
[88] H.-C. Um, J.-H. Jang, D.-H. Kim, C. Lee, Y.-J. Surh, Nitric oxide activates Nrf2 through S-nitrosylation of Keap1 in PC12 cells, Nitric oxide Biol. Chem. 25 (2011) 161–168.
[89] M.-H. Li, J.-H. Jang, H.-K. Na, Y.-N. Cha, Y.-J. Surh, Carbon monoxide produced by heme oxygenase-1 in response to nitrosative stress induces expression of glutamate-cysteine ligase in PC12 cells via activation of phosphatidylinositol 3-kinase and Nrf2 signaling, J. Biol. Chem. 282 (2007) 28577–28586.
[90] F. Nicoletti, P. Fagone, P. Meroni, J. McCubrey, K. Bendtzen, MTOR as a multifunctional therapeutic target in HIV infection, Drug Discov. Today (2011), https://doi.org/10.1016/j.drudis.2011.05.008.
[91] F. Nicoletti, et al., Inhibition of human immunodeficiency virus (HIV-1) infection in human peripheral blood leucocytes-SCID reconstituted mice by rapamycin, Clin. Exp. Immunol. (2009), https://doi.org/10.1111/j.1365-2249.2008.03780.x.
[92] D. Maksimovic-Ivanic, et al., HIV-protease inhibitors for the treatment of cancer: repositioning HIV protease inhibitors while developing more potent NO-hybridized derivatives? Int. J. Cancer (2017), https://doi.org/10.1002/ijc.30529.
[93] E. Lopez-Rivera, et al., Inducible nitric oxide synthase drives mTOR pathway activation and proliferation of human melanoma by reversible nitrosylation of TSC2, Cancer Res. 74 (2014) 1067–1078.
[94] D. Germanaud, et al., Level of viral load and antiretroviral resistance after 6 months of non-nucleoside reverse transcriptase inhibitor first-line treatment in HIV-1-

infected children in Mali, J. Antimicrob. Chemother. 65 (2010) 118–124.
[95] Katzenstein, D. A. & Holodniy, M. HIV viral load quantification, HIV resistance, and antiretroviral therapy. AIDS Clin. Rev. 277–303 at≤http://www.ncbi.nlm.nih.gov/pubmed/7488557 > .
[96] P.H. Groeneveld, et al., Increased production of nitric oxide correlates with viral load and activation of mononuclear phagocytes in HIV-infected patients, Scand. J. Infect. Dis. 28 (1996) 341–345.
[97] D. Torre, et al., Serum concentrations of nitrite in patients with HIV-1 infection, J. Clin. Pathol. 49 (1996) 574–576.
[98] G. Giovannoni, et al., Elevated cerebrospinal fluid and serum nitrate and nitrite levels in patients with central nervous system complications of HIV-1 infection: a correlation with blood-brain-barrier dysfunction, J. Neurol. Sci. 156 (1998) 53–58.